Journal of The Electrochemical Society, **149** (12) C637-C641 (2002)
0013-4651/2002/149(12)/C637/5/$7.00 © The Electrochemical Society, Inc.

Via Filling by Electrodeposition

Superconformal Silver and Copper and Conformal Nickel

D. Josell,[a,z] B. Baker,[a,*] C. Witt,[b] D. Wheeler,[a] and T. P. Moffat[a,*]

[a]*National Institute of Standards and Technology, Metallurgy Division, Gaithersburg, Maryland 20899, USA*
[b]*International Sematech, Austin, Texas, USA*

Superconformal deposition of silver in vias was studied. The observed experimental fill behavior is compared with predictions from a model based on the curvature-enhanced accelerator coverage mechanism of superconformal deposition. Superconformal copper deposition and conformal nickel deposition results are also modeled. The previously published model predicts via filling behavior using the dependence of deposition rate kinetics on the coverage of adsorbed catalyst. The requisite kinetic parameters are obtained from independent current-voltage and current-time transient studies conducted on planar substrates.
 [DOI: 10.1149/1.1517583]

Manuscript submitted January 30, 2002; revised manuscript received June 5, 2002. Available electronically October 24, 2002.

The use of electrodeposited copper in integrated circuits is due, in large part, to the ability of the deposition process to fill high-aspect-ratio features superconformally. This superconformal filling process was originally modeled, with only limited success, using traditional leveling-type theories involving depleted concentrations of deposition rate-inhibiting additives down the filling features.[1] The more recent curvature-enhanced accelerator coverage (CEAC) model has focused on competitive adsorption of deposition rate-inhibiting and catalyzing additives and conservation of the more strongly adsorbed catalyst during area change associated with metal deposition.[2-8] These models have predicted the initial ''incubation'' period of conformal deposition, the superconformal bottom-to-top filling itself, and the subsequent ''momentum'' plating bump formation over filled features that are commonly observed but which could not be explained by the leveling models.[9-11] Furthermore, these predictions were made with no fitting parameters; all kinetic factors were obtained from current-voltage studies with planar substrates in electrolytes containing a range of catalyst concentrations. An alternative model based on accumulation of catalyst at the bottoms of features has been published;[12] however, it required tuning of parameters to fit experimental fill results in order to model filling in a given electrolyte composition.

To date, papers that utilize CEAC-based models have detailed the agreement between predicted and experimental filling during copper[2-5] and silver[6] electrodeposition in trenches only. Superconformal deposition during iodine-catalyzed chemical vapor deposition of copper in vias[7] has been predicted using a CEAC-based model that describes superconformal filling of vias.[8] However, the work presented here is the first quantitative comparison of CEAC-based predictions and experiment for superconformal filling for the via geometry.

The model developed in Ref. 8 is used to describe superconformal filling of vias during both silver and copper electrodeposition in superfilling electrolytes. Because the vias being filled, with sidewalls canted by ~5°, are far from the idealized cylindrical structure envisioned in the model, nickel is also deposited conformally for comparison.

Experimental

Specimen fabrication.—A wafer, patterned with a repeating test structure, and including a copper seed, was provided by International Sematech. The test structure included rectangular blocks of vias, each containing vias of a single diameter between approximately 0.5 and 0.15 μm. The blocks were more than 3 mm long but ranged from 240 μm down to less than 10 μm wide, depending on the via diameter and spacing (pitch) within the block. Adjacent blocks were separated by an unpatterned region less than 10 μm wide. The pitch ranged from approximately 0.5 to 4 μm. The vias were patterned in 1 μm thick dielectric with a tantalum barrier layer and 100 nm thick sputter-deposited copper seed layer (thickness on the field outside the vias). The wafer was sectioned, in accordance with the periodic pattern, to obtain test specimens that were approximately 20×20 mm. Electrodeposition experiments at constant overpotential were conducted using these specimens in one of three electrolytes in order to obtain superconformal copper, superconformal silver, or conformal nickel deposits. The electrolyte compositions are detailed in Table I. Specimens were immersed in the electrolyte at the deposition voltage in order to avoid damage to the seed layer on the sidewalls of the vias. Standard three-electrode cells were used for all filling experiments. For the copper depositions, a copper anode and a saturated calumel reference electrode (SCE) were used. For the silver depositions, a platinum anode and a silver reference electrode were used. For the nickel depositions, a nickel anode was used (SCE). In all cases, the specimen was the cathode.

Specimens were inserted, and held during deposition, in a vertical position such that buoyancy-driven convection arising from the concentration gradient near the surface would be expected to induce formation of a boundary layer during deposition. The specimens were removed from the electrolyte after predetermined deposition times, rinsed in deionized water, and dried. They were then cross-sectioned for viewing by scanning electron microscope using standard techniques.

Filling vias.—Figure 1 shows a series of cross-sectioned vias, obtained by scanning electron microscope, that detail the filling process during copper electrodeposition in the largest features studied. The images, reflecting the fill profiles obtained at successive 10 s intervals, were obtained by interrupting electrodeposition on each specimen after the indicated deposition time. The copper deposition is conformal during the first 60 s. Deposition on the bottom surface accelerates at ~70 s and superconformal bottom-to-top filling occurs. Figure 2 shows a similar set of images obtained during silver electrodeposition. The silver deposition is also initially conformal, with rapid bottom-to-top filling starting at ~40 s. A series of images obtained during the period when the rapid bottom-to-top filling occurs is shown in Fig. 3; the significant difference in the deposition (growth) rates on the bottom and sidewall surfaces that characterizes the superconformal deposition process is clear. The time dependence of the feature filling obtained through conformal nickel deposition in the same patterned vias is detailed in Fig. 4. Growth is conformal from start to finish, resulting in a v-notch surface profile whose internal angle reflects the tilt of the original sidewalls.

Quantifying the deposition.—The time-dependent thicknesses of the metal deposits on the via base, obtained from cross-sectioned specimens including those shown in Fig. 1-3, are summarized in Fig. 5 for the copper and Fig. 6 for the silver deposits. In both cases

* Electrochemical Society Active Member.
z E-mail: daniel.josell@nist.gov

Table I. Constituent concentrations of the silver,[6] copper,[5] and nickel electrolytes.[a]

Metal	Electrolyte compositions
Silver	0.34 mol/L $KAg(CN)_2$ + 2.3 mol/L KCN + proprietary[a]
Copper	0.25 mol/L $CuSO_4 \cdot 5H_2O$ + 1.8 mol/L H_2SO_4 + 1×10^{-3} mol/L NaCl + 88.2×10^{-6} mol/LH $(OCH_2CH_2)_{55}OH$ + 6.4×10^{-6} mol/L $Na_2(SO_3(CH_2)_3S)_2$
Nickel	1.5 mol/L $Ni(SO_3NH_2)_2$ + 0.5 mol/L H_3BO_3

[a] Additives in the ''Techni-Silver E'' electrolyte from Technic, Inc., are not disclosed. Note that corporate and product names are provided for experimental accuracy. They do not imply NIST endorsement.

the deposits are initially conformal, as reflected in the equal deposition rates on the bottoms and sidewalls of the vias. At later times, the silver and copper deposit more rapidly on the bottom surfaces than on the sidewalls, resulting in bottom-to-top filling characteristic of superconformal deposition. For the silver, the uncertainty (2σ) of measurements during the conformal growth period is ± 0.03 μm. This value reflects surface roughness and measurement resolution. Once bottom-up filling begins, the data scatter increases to ± 0.25 μm for all partially filled vias. This value represents measured variations across individual specimens. For the ~10 s period of superconformal growth, a ± 2 s variation in when superconformal filling begins (*i.e.*, the duration of the incubation period) could provide the observed variation. Such a variation in the ~40 s incubation period would result from a $\pm 5\%$ variation in boundary layer thickness, for example.

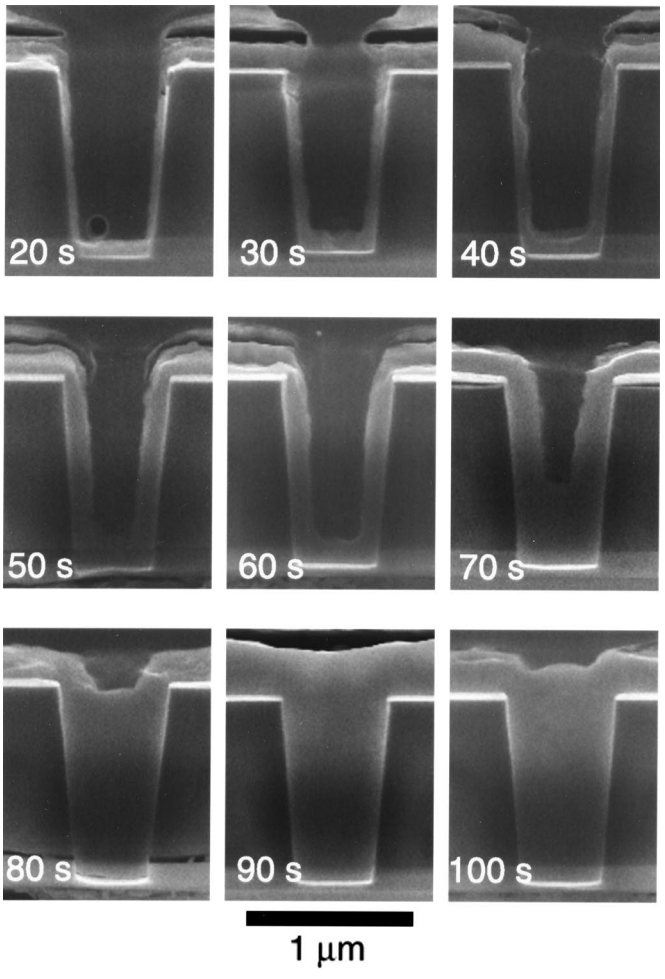

Figure 1. Vias cross-sectioned after copper deposition for the indicated periods of time at −0.2 V overpotential (SCE). The process of feature filling is captured at 10 s intervals. Note that filling accelerates after approximately 70 s, with the bottom surface moving up more than half the height of the via during the following 10 s interval. The thickness of the deposit outside the vias includes a copper seed over the (bright) tantalum layer. Specimen preparation resulted in smearing of the tantalum layer in specimens with 20 and 60 s of deposit. These vias were in square arrays with via spacings of ~4 μm.

Modeling

Predicted curves are superimposed on Fig. 5 and 6 for vias with aspect ratios (height/diameter) of 1.6 and 2.2. These aspect ratios correspond to those of vias that are 1 μm high with diameters equal to those at the tops and bottoms, respectively, of the experimental vias. The predictions were obtained using the CEAC-based model of superconformal deposition in vias published in Ref. 8. All the kinetic parameters used in the modeling are shown in Table II; they come from Ref. 6 for the silver and Ref. 5 for the copper. They were obtained entirely from studies of the deposition behavior on planar substrates in both cases. There are no fitting parameters. The electrolytes were comprised of aquo $-Ag^+$ and Cu^{2+} ions; thus, two electrons of charge transfer correspond to electrodeposition of two silver atoms or one copper atom, respectively. The simulations predict the conformal growth period, the rapid change to superconfor-

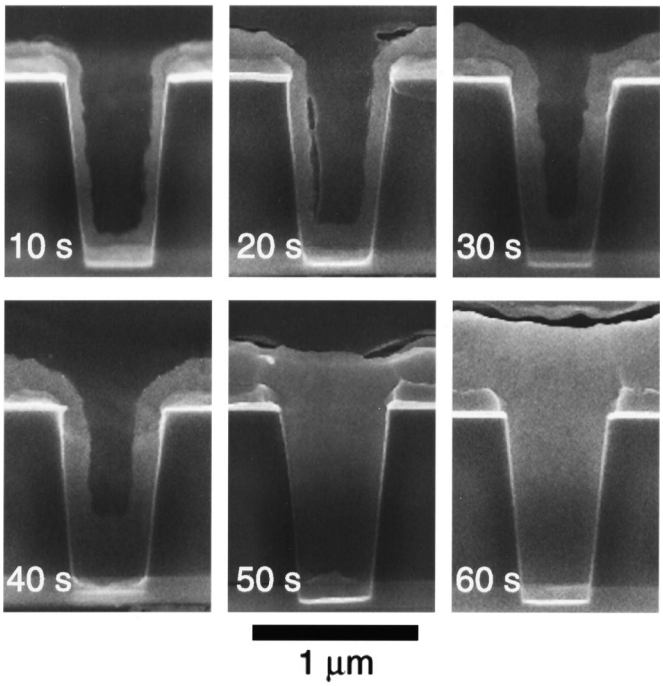

Figure 2. Vias cross-sectioned after silver deposition for the indicated periods of time at −0.485 V overpotential *vs.* silver. The process of feature filling is captured at 10 s intervals. Note that filling accelerates at approximately 40 s, with the bottom surface moving up more than half the height of the via during the following 10 s interval. The copper seed is visible between the (bright) tantalum layer and the silver deposit outside each via. These vias were in square arrays with via spacings of ~2 μm.

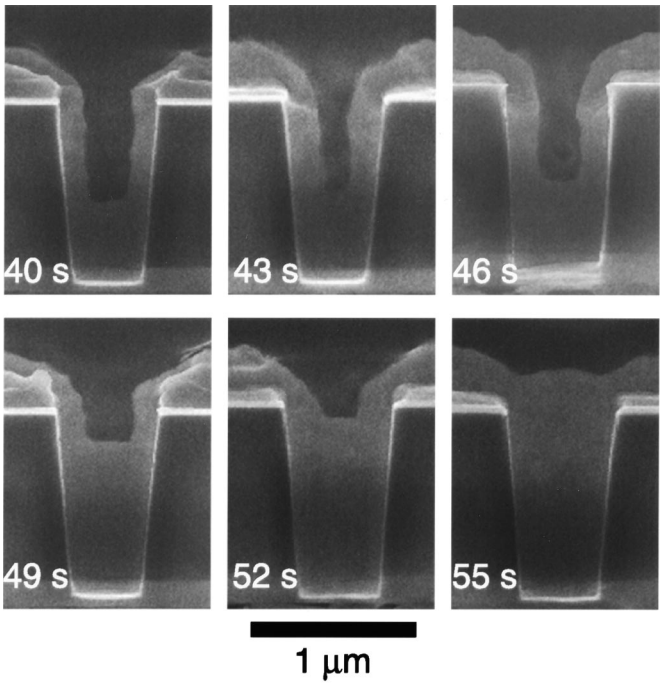

Figure 3. Vias cross-sectioned after silver deposition for the indicated periods of time at −0.485 V overpotential *vs.* Ag. The superconformal filling of the via is captured at 3 s intervals. These vias were in square arrays with via spacings of ~2 μm.

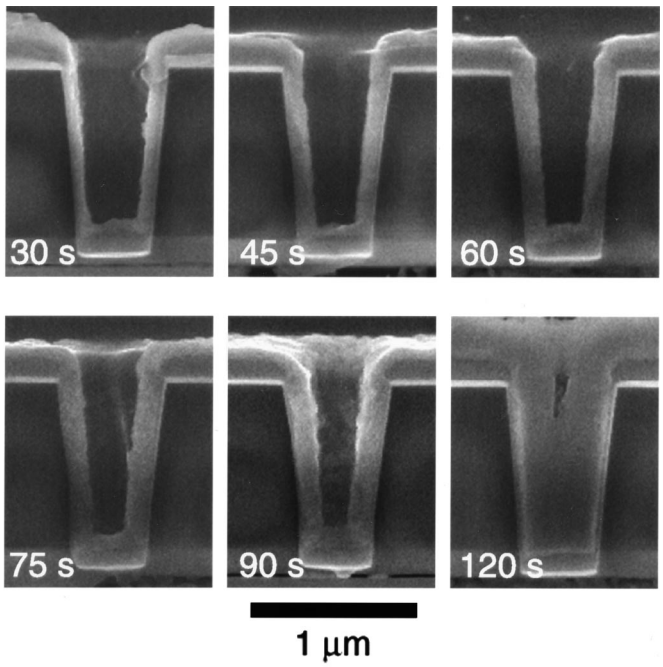

Figure 4. Vias cross-sectioned after nickel deposition for the indicated periods of time at −1.42 V SCE. The conformal filling of the via is captured at 15 s intervals, with the notch manifesting geometrical leveling from the sloping sidewalls visible in the final image (after a 30 s interval). These vias were in a square array with feature spacing of ~2 μm. Smearing of the nickel deposits during specimen preparation is visible on the surface outside the via with 30 s of deposition.

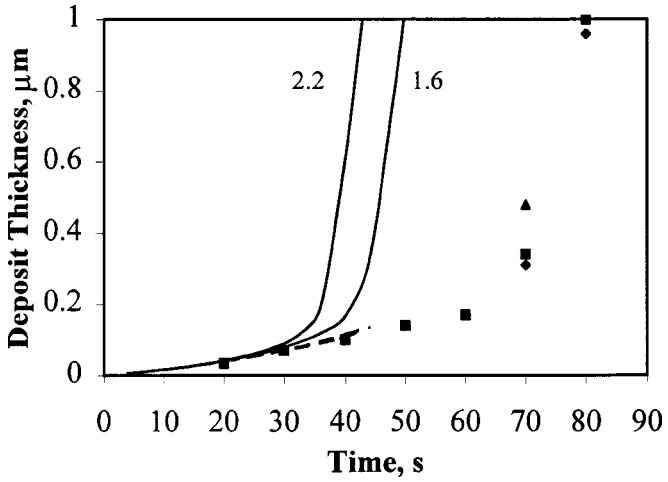

Figure 5. The time-dependent thickness of the copper deposit on the bottoms of the filling vias. (◆, ■, ▲) Data for vias spaced 1, 2, or 4 μm apart, respectively. The sidewall deposits thicken, throughout via filling, at essentially the same rate as the deposits on the bottom surface during the first 60 s. Deposit thicknesses predicted by the model[8] for isolated vias, using the parameters in Table II, are shown for two aspect ratios that span the dimensions of the nonideal vias. (——) The predicted thicknesses on the bottom surface. (— — —) Predicted thickness on the sidewalls. The aspect ratio of the via being modeled is indicated next to the corresponding solid curve; the dashed curves are distinguishable only from where they terminate (*i.e.*, when the bottom surface escapes the via).

mal filling, and within measurement uncertainty, the duration of the superconformal growth period. The predicted conformal growth periods are, however, significantly shorter than the experimental values. Note that although this particular model does not address the latter stage of deposition, other CEAC-based models predict bump formation over filled features such as observed here (Fig. 3).

Figure 7 shows the predictions for the conformal nickel deposition. The predictions prior to sidewall impingment are based on a time- and location-independent growth velocity of $v_o = 0.0026$ μm/s obtained from the 0.31 μm sidewall thickness at 120 s (Fig. 4). The time τ_i before the sidewalls impinge is given by $\tau_i \approx R/v_o$, where R is the radius at the bottom of the via. For

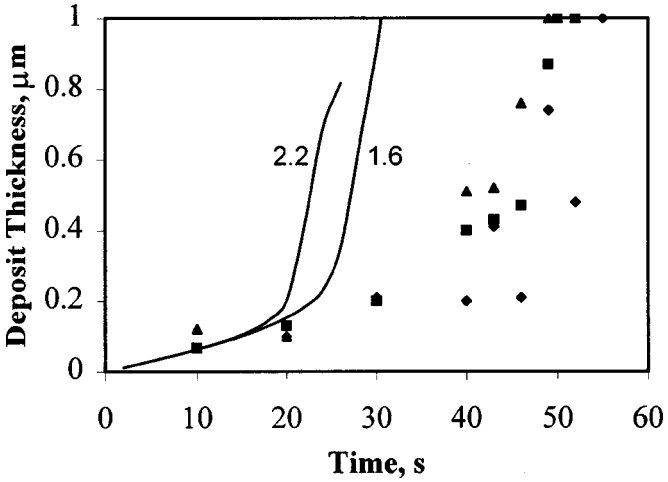

Figure 6. The time-dependent thickness of the silver deposit on the bottoms of the filling vias. (◆, ■, ▲) Data for the vias spaced 1, 2, or 4 μm apart, respectively. Deposit thicknesses on the bottoms of isolated vias predicted by the model[8] using the parameters in Table II are shown (——) for two aspect ratios that span the dimensions of the nonideal vias. The aspect ratio of the via being modeled is indicated next to the corresponding solid curve.

Table II. Parameters for the modeling of superconformal deposition of silver and copper from Ref. 6 and 5, respectively.

Metal	Ω (cm^3/mol)	δ μm	$D_{catalyst}$ (cm^2/s)	$D_{metal\ Ion}$ (cm^2/s)	Γ (mol/cm^2)	$k(\eta)$ [or $k'(\eta)$] (cm^3/mol s)	α	i_o (mA/cm^2)
Silver	10.3	135	4.5×10^{-6}	7.6×10^{-6}	7.6×10^{-10}	$5.2 \times 10^4 + 5.1 \times 10^6\eta^2$	$0.17 + 0.11\theta$	$0.32 + 0.86\theta$
Copper	7.1	150	5×10^{-6}	1×10^{-5}	9.7×10^{-10}	$1.8 \times 10^5 - 2.7 \times 10^7\eta^3$	$0.45 + 0.30\theta$	$0.069 + 0.64\theta$
T = 298 K		R_B = 8.314 J/mol K			F = 96485 C/mol			

R = 0.25 μm, impingment occurs at $\tau_i \approx 96$ s. After the sidewalls impinge, the upward velocity of the bottom of the resulting notch is given by $v_o/\sin(\theta)$, where θ is the outward tilt of the sidewalls from vertical. This is a manifestation of geometrical leveling. Because the tilt angle is small, $\theta \approx 5°$, the upward velocity after impingement is comparatively high, and the resulting predictions are sensitive to both v_o and θ. A value of v_o that is 5% higher, or a value of tilt angle that is 1° smaller, is all that is required to make the prediction agree with the measured height of the notch at 120 s. Both changes are within measurement uncertainty.

Discussion

It appears unlikely that the CEAC mechanism is not the phenomenon underlying the superfilling of the vias: the model predicts the conformal deposition followed by the superconformal deposition, including the relatively sharp transition between the two, and within measurement error, the duration of the superconformal growth period, all with no fitting parameters. Several factors that could affect the duration of the conformal growth period, for which predictions underestimate the experimental results, are described in what follows. The CEAC-based models that have been quantitatively successful in predicting the geometry of superconformal filling in trenches, also with no fitting parameters, have not examined the time dependence of filling as done here.

Approximations and Uncertainties

The model itself.—The particular CEAC-based model used here contains several approximations, including an assumption of instantaneous redistribution on the bottom surface of catalyst that had been adsorbed on eliminated sidewall area. The impact of these approximations on the period of conformal growth is unclear, as an exact solution for this geometry does not presently exist to allow comparison.

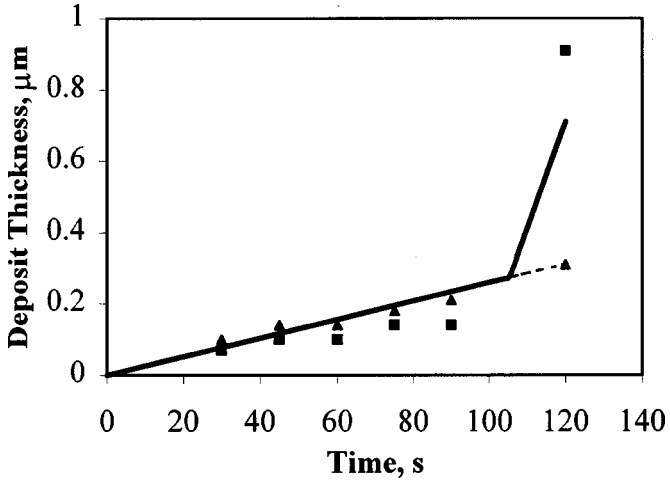

Figure 7. The time-dependent thickness of the nickel deposit on the bottoms and sidewalls of the filling vias. The different thicknesses measured from (■) the bottoms and (▲) sidewalls prior to 100 s are likely due to the difficulty of discriminating between the copper seed and nickel electrodeposit within the features. (- - - -) Linear growth rate determined from the sidewall thickness measured at 120 s. (——) The associated prediction for the height of the bottom surface, obtained for sidewalls tilting outward 5° from vertical.

Feature density.—Feature density does impact the time before the rapid upward filling begins (Fig. 5 and 6). That the delay increases with pattern density implies that this is a manifestation of either/both metal ion or catalyst depletion over the features. Though the model includes composition gradients of the metal ion and catalyst across the boundary layer, these gradients are determined by balancing the fluxes across the boundary layer with those attaching to a planar surface. Metal deposition and/or catalyst adsorption on the additional surface area associated with the sidewalls evidently leads to a significant increase in the magnitude of the gradient and associated drop in the concentrations at the specimen surface. Initially, the additional surface area responsible for this effect is expressed using the factor ψ

$$\psi = 1 + \frac{2\pi Rh}{d^2} \quad [1]$$

which equals the actual surface area divided by the planar area, given via radius R, via spacing d, and via height h. For a flat surface ($d \to \infty$), $\psi = 1$. For the 1 μm deep vias, using an average radius of 0.25 μm, $\psi = 1.1$ for the 4 μm via spacing, $\psi = 1.4$ for the 2 μm via spacing, and $\psi = 2.6$ for the 1 μm via spacing.

An approximate mass balance equation representing equality of the metal ions diffusing across the boundary layer with the rate of metal deposition, for the nonplanar surface, is expressed as follows. In terms of the metal ion concentration drop from the bulk electrolyte concentration, C_{bulk}, to that at the top of the feature, C_{top}, for boundary layer thickness δ, atomic volume Ω_M, and diffusion coefficient D_M, one can write

$$\psi v_o = \Omega_M D_M \frac{C_{bulk} - C_{top}}{\delta} \quad [2]$$

This presumes spatially uniform deposition rate v_o, ignoring composition gradients within the via,[3-5] and only applies prior to the start of superconformal deposition. A similar analysis can be done for the impact of increased surface area on the accumulation of catalyst. When accumulation is diffusion limited, so that $C_{top} \ll C_{bulk}$, the right side is nearly constant and the deposition rate v_o scales inversely to ψ. The incubation time for the inception of bottom-up filling thus scales with ψ. Under such conditions, Eq. 2 predicts that the incubation times for the vias with 4 μm spacing will be only ~10% longer than those for isolated vias, while those with 2 μm spacing will be ~40% longer, and those with 1 μm spacing will be ~160% longer. These effects are less pronounced when interface kinetics play a significant role in limiting either metal deposition or catalyst adsorption, such as is the case for both the silver and copper depositions. As would be expected from these results, the experimental data for the vias with 4 μm spacing lie closest to the curves (Fig. 5 and 6), which are predictions for isolated vias.

Depletion over the experimental regions due to consumption from the global distribution of vias, rather than the local ψ, is also likely. This is of particular concern because the distance between patterned blocks, and the sizes of some blocks (noted earlier), are

significantly smaller than the anticipated 135-150 μm boundary layer thickness. Furthermore, ψ for some blocks is significantly higher than the values noted previously. Indeed, the general increase of deposition times beyond the predicted values for all via spacings as well as the relatively small impact of via spacing on deposition times are both consistent with such a global depletion effect.

The spatially periodic geometry does lend itself to quantitative analysis through the calculus of partial differential equations with boundary values. Such analysis has been done, for example, to study the impact of spatially varying area for deposition (achieved by local variation of coverage with photoresist) on the electrical potential and resulting deposition.[13] Variations of feature density on the wafer, or specimen, scale require an additional level of calculation to deal with concentration variations as electrolyte moves over regions of varying pattern density.[14,15]

Incorrect or inappropriate kinetics.—The parameters used for the copper fill modeling are for electrolyte containing the additive 3-mercapto-1-propanosulfonate (MPSA) rather than the dimer version bis-(sodium sulfopropyl)-disulfide (SPS) actually used in the experiments. They were obtained from analysis of hysteresis in cyclic current-voltage experiments conducted on planar substrates in electrolytes containing various concentrations of MPSA.[5] To account for the dimer nature of SPS, an MPSA concentration of twice the experimental SPS concentration was used in the modeling. The relevant parameters for the electrolyte with SPS are not presently available; it is, however, known that the kinetics for adsorption of SPS from the electrolyte are slower than for MPSA (as quantified by the factor $k(\eta)$ in Table II).[16] Slower deposition, and associated area reduction, would be expected to lead to a longer conformal growth period, possibly explaining the discrepancy in the incubation period. For the silver deposition, in light of the significant unknowns about the composition of the proprietary electrolyte, it is possible that the associated kinetic parameters in Table II are also inaccurate.

Incorrect boundary layer thickness.—Spatial and temporal variation of boundary layer thickness can be significant for a vertical specimen in an unstirred solution like that used in these experiments, as well as in the studies on planar substrates used to obtain the kinetic parameters. Indeed, for an electrolyte of similar composition to that for copper in Table I (without additives), the local current decreases monotonically with increasing height on the specimen, with a fractional decrease of ~40% going up the first 1 cm from the specimen bottom and an additional ~20% going up the next cm.[17] Specimen-to-specimen variation arising from this effect was reduced in these experiments through the study of only those features located at and less than 3 mm above the specimen midplane (*i.e.*, 1-1.3 cm above the specimen bottom). However, accurate assessment and application of the kinetics with a CEAC-based model, as with any other model, requires control of the boundary layer thickness, *e.g.*, through a rotating disk geometry. There is no significant spatial variation of the potential for the specimen geometry and deposition conditions used here.

Nonideal via geometry.—The nonvertical sidewalls of the patterned via make the model in Ref. 8, with its vertical sidewalls, an approximation of the experiments actually being modeled. Due to the sloping sidewalls, the area of the bottom surface increases as it moves upward. This offsets the area decrease that is associated with the filling of the feature. According to the CEAC model, this leads to a decrease of the catalyst coverage on that surface and an extended incubation period. However, this would have the greatest effect when the bottom surface is moving up significantly, experiencing the changing radius, as during the period of superconformal deposition. It would not be expected to substantially extend the incubation period.

Conclusions

Filling of vias with silver, copper, and nickel was studied experimentally and then modeled. Feature filling during both copper and silver deposition exhibits the bottom-to-top deposition characteristic of superconformal growth. Feature filling during the nickel deposition occurs through geometrical leveling with no evidence of superconformal filling behavior. A model based on the CEAC mechanism of superconformal deposition was used to predict the superconformal filling with copper and silver. As with previous applications of CEAC-based models describing superconformal deposition in trenches, the predictions for superconformal filling of vias are based entirely on kinetics obtained from studies of deposition on planar specimens. The model predicts the superconformal filling behavior, including an incubation period of conformal growth and subsequent superconformal bottom-to-top filling. Possible explanations for the underestimated duration of the incubation period were detailed.

The National Institute of Standards and Technology assisted in meeting the publication costs of this article.

References

1. P. C. Andricacos, C. Uzoh, J. O. Dukovic, J. Horkans, and H. Deligianni, *IBM J. Res. Dev.*, **42**, 567 (1998).
2. T. P. Moffat, D. Wheeler, W. H. Huber, and D. Josell, *Electrochem. Solid-State Lett.*, **4**, C26 (2001).
3. D. Josell, D. Wheeler, W. H. Huber, and T. P. Moffat, *Phys. Rev. Lett.*, **87**, 016102 (2001).
4. D. Wheeler, D. Josell, and T. P. Moffat, Submitted for publication.
5. D. Josell, D. Wheeler, W. H. Huber, J. E. Bonevich, and T. P. Moffat, *J. Electrochem. Soc.*, **148**, C767 (2001).
6. T. P. Moffat, B. Baker, D. Wheeler, J. E. Bonevich, M. Edelstein, D. R. Kelly, L. Gan, G. R. Stafford, P. J. Chen, W. F. Egelhoff, and D. Josell, *J. Electrochem. Soc.*, **149**, C423 (2002).
7. D. Josell, D. Wheeler, and T. P. Moffat, *Electrochem. Solid-State Lett.*, **5**, C44 (2002).
8. D. Josell, D. Wheeler, and T. P. Moffat, *Electrochem. Solid-State Lett.*, **5**, C49 (2002).
9. J. Reid and S. Mayer, in *Advanced Metallization Conference 1999*, p. 53, M. E. Gross, T. Gessner, N. Kobayashi, and Y. Yasuda, Editors, MRS, Warrendale, PA (2000).
10. T. Ritzdorf, D. Fulton, and L. Chen, in *Advanced Metallization Conference 1999*, p. 101, M. E. Gross, T. Gessner, N. Kobayashi, and Y. Yasuda, Editors, MRS, Warrendale, PA (2000).
11. E. Richard, I. Vervoort, S. H. Brongersma, H. Bender, G. Beyer, R Palmas, S Lagrange, and K. Maex, in *Advanced Metallization Conference 1999*, p. 149, M. E. Gross, T. Gessner, N. Kobayashi, and Y. Yasuda, Editors, MRS, Warrendale, PA (2000).
12. A. C. West, S. Mayer, and J. Reid, *Electrochem. Solid-State Lett.*, **4**, C50 (2001).
13. J. O. Dukovic, in *Advances in Electrochemical Science and Engineering*, Vol. 3, H. Gerischer and C. W. Tobias, Editors, p. 117, VCH Publishers, New York (1994).
14. M. O. Bloomfield, S. Sen, K. E. Jansen, and T. S. Cale, in *The 18th International VLSI Multilevel Interconnection Conference Proceedings*, p. 397, Santa Clara, CA, Sept 25-26, 2001.
15. M. O. Bloomfield, S. Soukane, K. E. Jansen, and T. S. Cale, in *Semiconductor Technology*, M. Yang, Editor, PV 2001-17, p. 94, The Electrochemical Society Proceedings Series, Pennington, NJ (2001).
16. Authors' preliminary, unpublished results.
17. C. R. Wilke, M. Eisenbert, and C. W. Tobias, *J. Electrochem. Soc.*, **100**, 513 (1953).